Proton NMR Relaxation Study on the Nematic Nematic Phase Transition in A131 Liquid Crystal

7 **AUTHORS**, INCLUDING:

Alina Aluculesei
Foundation for Research and Technology - Hel…
9 PUBLICATIONS **73** CITATIONS

Fabian Vaca Chavez
National University of Cordoba, Argentina
34 PUBLICATIONS **461** CITATIONS

Pedro José Sebastião
University of Lisbon
76 PUBLICATIONS **547** CITATIONS

Ronald Y Dong
University of British Columbia - Vancouver
220 PUBLICATIONS **2,278** CITATIONS

Proton NMR Relaxation Study on the Nematic–Nematic Phase Transition in A131 Liquid Crystal

A. Aluculesei,[†,‡] F. Vaca Chávez,[‡] C. Cruz,[†,‡] P. J. Sebastião,*[,†,‡] N. G. Nagaveni,[§] V. Prasad,[§] and R. Y. Dong[∥]

[†]Department of Physics, Instituto Superior Técnico, Technical University of Lisbon, Av. Rovisco Pais, 1049-001 Lisbon, Portugal
[‡]Centro de Física da Matéria Condensada, Av. Prof. Gama Pinto 2, 1649-003 Lisbon, Portugal
[§]Center for Soft Matter Research, P.O. Box 1329, Jalahalli, Bangalore 560 013, India
[∥]Department of Physics and Astronomy, University of British Columbia, Vancouver, BC V6T 1Z1, Canada

Ⓢ Supporting Information

ABSTRACT: A study of the proton NMR spin–lattice relaxation time, T_1, of the A131 liquid crystal compound as a function of temperature and Larmor frequency, using a combination of fast field-cycling and standard NMR techniques, is presented. The frequency dispersion in a wide range (from 10 kHz to 300 MHz) at different temperatures and the temperature variation of T_1, in several frequency conditions, were analyzed considering the contributions of the molecular movements generally detected in liquid crystals. In the case of nematic phases of calamitic liquid crystals, the nuclear spin relaxation is dominated by collective movements and local molecular reorientations. The experimental results clearly show a transition within the nematic range of this compound, previously identified as one from the uniaxial to the biaxial phase. This transition can be associated with a slowing down of the molecular rotations around the long molecular axis, where the preferred orientation defines the principal director as detected in the T_1 dispersion analysis.
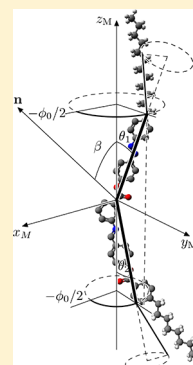
■ INTRODUCTION

The synthesis of bent-core liquid crystals has significantly enlarged the existing set of mesophases exhibited by thermotropic liquid crystals. The distinctive molecular structure of these compounds, also called "banana shape", introduces additional symmetry properties to the local packing of the mesogenic units giving rise to a completely new set of lamellar mesophases (called the B phases).[1] Most of the interest in these systems (whose peculiar phases were first reported in 1996 and primarily approached theoretically in 1983)[2,3] experienced a remarkable burst since the end of the twentieth century due to their unique electrically switching properties. The fact that some of the B phases exhibit ferroelectric properties opened perspectives of applications in the display industry.

Aside from the newly found lamellar B phases, some of the nematic phases exhibited by bent-core mesogens, maybe not so surprisingly, also showed very peculiar behaviors. These features are due to the possibility of rotational symmetry breaking (at least locally) in the plane perpendicular to the main nematic director as a consequence of the bent-shape structure of the molecular cores. Actually, bent-core and related compounds were among the first of a number of liquid-crystalline systems where experimental indication of biaxial nematic order has been found recently.[4–7]

The theoretical prediction of the biaxial nematic (N_b) phase happened quite a long time ago, in 1970 by Freiser,[8] and this type of mesophase was first observed in a lyotropic liquid crystal by Yu and Saupe in 1980.[9] Nevertheless, the design, synthesis, and identification of thermotropic liquid crystals exhibiting biaxial nematic phases have remained for decades a challenge for synthetic chemists, experimental physicists, and theoreticians.[10–14] Recently, a number of experimental results, obtained through different techniques, seem to point in different directions with respect to the recognition of the biaxial nematic ordering in the bent-core A131 compound.

In 2005, Prasad and co-workers clearly identified a nematic–nematic phase transition in that compound by means of POM and synchrotron X-ray scattering.[6] The molecular structure and the phase sequence reported for this compound are shown in Figure 1. The experimental findings, namely the anisotropy of the
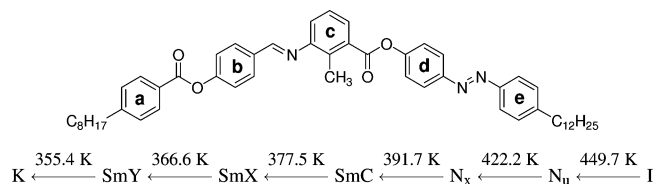
Figure 1. A131 chemical structure and polymorphism. N_x stands for a second nematic phase found between the uniaxial N_u phase and the SmC phase as explained in the text.

small-angle X-ray pattern and the remarkable distinction of the temperature dependence of the positional order correlation lengths in the two nematic temperature domains, are fully compatible with a second-order N_u–N_b transition. These experimental results were found to agree with the temperature-dependent ^{13}C NMR measurements reported in 2007, in which the determination of order parameters of different molecular segments was obtained through the analysis of the chemical shift anisotropy (CSA) tensors.[15] Calculation of the chemical shielding tensor (CST) obtained in a study by means of density functional theory (DFT) and respective comparison with the CSA tensors measured by the two dimensional (2D)-NMR SUPER technique were used to assist the assignment of ^{13}C peaks, which were in reasonable agreement with previous results on this system.[16] This technique allowed the nematic S and $D \equiv S_{xx} - S_{yy}$ order parameters for each of the five aromatic rings of A131 to be obtained.

However, results of electro-optical measurements on homeo-tropically aligned samples were reported in 2009 by Takezoe and co-workers to indicate that the observed nematic phase of A131 is of uniaxial nature in the full temperature range.[17] The argument presented focuses on the defect structure observed in the plane of the cell (perpendicular to the main nematic director) which always vanishes for sufficiently high electric fields. According to the authors, the existence of nematic biaxiality should prevent this effect since the anisotropy of secondary directors would remain, regardless of the intensity of the applied electric field in the direction of the main director. Two subsequent papers by different authors report contradictory results of electro-optical measurements on this system.[18,19] In those studies where the biaxial nematic phase is not observed, their results have been identified as anchoring transitions, instead of the assigned N_u–N_b phase transition. The "SmC-like" pattern observed in the small-angle X-ray diffraction pattern is thought to be due to the existence of smectic clusters (or cybotactic nematic) in the whole temperature range previously attributed to the biaxial nematic phase.

Independent of the question regarding assignment of the biaxial label to the lower-temperature nematic phase initially observed in 2005 between the N_u and SmC phases,[6] it seems rather interesting to investigate the nature of this nematic–nematic transition and the reasons behind the clear differences observed by different experimental techniques in the two temperature domains. It is worthwhile to remember that different types of nematic phases and nematic–nematic transitions have been recently observed and are raising considerable research interest in systems of relative molecular simplicity.[5,7,20–23] In fact, besides the clear technological impact of these new variants of the nematic phase, the alternative types of molecular organization that give rise to the nematic–nematic transitons remain an open question.[22–24] In our view, the problem of the N–N transition in A131 also deserves a detailed discussion in order to approach a better understanding of this type of bent-core mesogen. The purpose of this paper is to present results by means of a different experimental technique to contribute to that debate. Proton NMR relaxation is a powerful technique to deal with molecular movements in a very wide range of characteristic times, providing that a suitable combination between standard and fast field-cycling NMR techniques is used.[25,26] Molecular motions of different time scales are accessed by scanning the proton spin–lattice relaxation time, T_1, over a range of Larmor frequencies associated with the inverse of these characteristic times. In that way, different mesophases will show

variations of the T_1 frequency dispersions, which are strongly influenced by the molecular organization corresponding with their characteristic molecular packings. The compound A131 studied here exhibits a very rich polymesomorphism, including two nematic phases and three smectic phases, SmC, SmX, and SmY.[6] In this study, particular attention will be given to the nematic–nematic transition and also to the SmC phase that follows the low-temperature nematic phase, herein called N_x.

■ EXPERIMENTAL SECTION AND RESULTS

A sample of 300 mg of A131[6] was sealed, under moderate vacuum, in a standard 5 mm NMR tube. In the NMR probe, the sample temperature was regulated to better than ± 0.5 K using air flow.

The ^{1}H spin–lattice relaxation time was measured as a function of temperature and of the Larmor frequency $\nu_L = \omega_L/2\pi$ using three different NMR instruments. The low-frequency measurements between 8 kHz and 9 MHz were made using a home-developed fast field-cycling NMR relaxometer.[27] This experimental technique allows for the T_1 measurement, using the classical inversion–recovery pulse sequence, at frequencies usually inaccessible by standard NMR spectrometers. This is possible because the magnetic field in the equipment used is switched up and down between two values: a fixed high value corresponding to the signal acquisition radiofrequency of 8.9 MHz and a variable low value at which the relaxation time is to be measured.[27–29]

A variable field electromagnet and a 7T superconducting magnet were used in conjunction with a Bruker Avance II NMR console for measurements at Larmor frequencies between 10–100 and at 300 MHz, respectively. The T_1 measurements were made using the inversion–recovery pulse sequence with phase cycling to compensate for any dc-bias components in the free induction decay (FID) signal.

The spin–lattice relaxation measurements were made after slowly cooling the sample, at a rate of 1 K/min from the iso-tropic phase to the desired temperature in each mesophase. T_1^{-1} dispersions were obtained at temperatures of 438, 429, 425, 412, 410, and 406 K in the nematic phases and 379 K in the SmC phase. In addition, detailed temperature-dependent profiles were obtained in the nematic and SmC phases for six different Larmor frequencies: 90, 9, and 1 MHz and 100, 20, and 10 kHz. Some of the experimental results are presented in Figures 2 and 3. The remaining experimental results are presented in the Supporting Information.

As can be observed in Figure 2, the T_1^{-1} temperature dependence is similar in the case of the Larmor frequencies above the megahertz range and presents some interesting differences at lower frequencies, in particular at 20 and 10 kHz (see Figure 2b). In fact, in the case of Larmor frequencies below 100 kHz, the spin–lattice relaxation results suggest some fluctuations around 422.2 K and an increase of T_1^{-1} with decreasing temperature below 391.7 K. These particular temperatures have been identified by DSC (see traces in the Supporting Information) as the N–N and N–SmC phase transition temperatures. The differences observed between the T_1 values in the N and SmC phases are also detected in the T_1^{-1} dispersions presented in Figure 3. In this figure, the longitudinal relaxation rate is clearly different at 379 K; some differences can also be observed in the intermediate frequency range between 500 kHz and 50 MHz.

The T_1^{-1} dispersion profiles observed in the A131 nematic phases are identical to those obtained for nematic phases of other biphenyl and triphenyl liquid crystals.[25,26,30] However, the T_1^{-1}
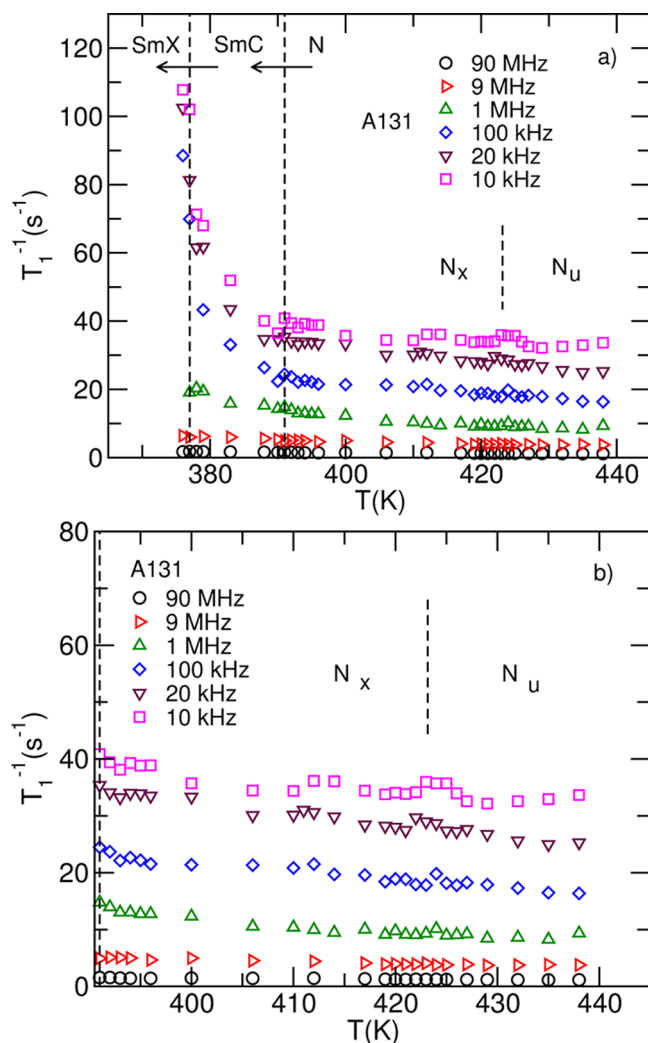
Figure 2. Spin−lattice relaxation rate as a function of temperature for six selected frequencies, as explained in the text. (a) $T_1^{-1}(T)$ in the SmC, N_x, and N_u temperature domains. (b) Detailed $T_1^{-1}(T)$ in the N_x and N_u temperature domains.
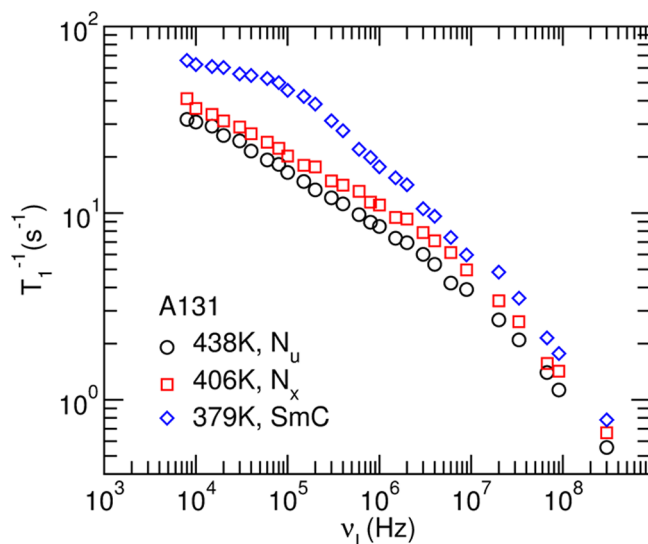
Figure 3. Spin−lattice relaxation rate as function of the Larmor frequency for three selected temperatures, as explained in the text.

fluctuations observed around the N−N phase transition for frequencies below 1 MHz might reflect the influence of changes of molecular order or changes of local molecular packing on the collective motions relaxation process, or both, as this relaxation mechanism has been found to be the dominant one at low frequencies.

■ RELAXATION MODELS AND DATA ANALYSIS

Relaxation Mechanisms and Models. The relaxation rate T_1^{-1} is usually assumed to be described by a linear combination of statistically independent contributions, each one associated with specific types of molecular motions. It is also commonly observed that cross-terms can be neglected, as the characteristic correlation times associated with those motions are considerably different. The total relaxation rate can then be expressed as

$$\left(\frac{1}{T_1}\right) = \left(\frac{1}{T_1}\right)_{SD} + \left(\frac{1}{T_1}\right)_{C} + \left(\frac{1}{T_1}\right)_{R} \tag{1}$$

where SD, C, and R stand for translational self-diffusion, collective motions, and local molecular rotations/reorientations, respectively.

In some cases, additional distinction in the contribution(s) can even be considered, as it happens, for instance, when chain rotations have correlation times of a different order of magnitude versus those associated with the slower core rotations/reorientations. Also, the collective motions in the case of SmC phases can include contributions from both layer undulations and in-plane fluctuations of the tilt direction.[31] The proton T_1^{-1} can be expressed in terms of the spectral densities that reflect the modulation by motions of the interspin dipolar interactions between either intra- or intermolecular spins.

The main relaxation mechanisms considered for the analysis of the proton spin−lattice relaxation in this work are provided below.

(i) Translational self-diffusion is described by the model proposed for nematics by Žumer and Vilfan.[32] This contribution can be approximated by the analytical expression obtained by Torrey for the isotropic phase[33] with a correction factor of $1/1.4$[32]

$$\left(\frac{1}{T_1}\right)_{SD} \simeq \frac{1}{1.4} C_d \frac{n\tau_D}{d^3}[\mathcal{T}(\alpha, \omega\tau_D) + 4\mathcal{T}(\alpha, 2\omega\tau_D)] \tag{2}$$

where $C_d = (1/2)[3\mu_0\gamma^2\hbar/(8\pi)]^2$ is the strength of the dipolar interaction, $\mathcal{T}(\alpha,\omega\tau_D)$ is a dimensionless analytical function that depends on the average time τ_D between diffusion jumps, α is related to the mean-square jump distance $\langle r^2 \rangle$, the self-diffusion constant, D, and the molecular width, d, by the relation $\langle r^2 \rangle = 12\alpha d^2 = 6\tau_D D$, and n is the density of ^1H spins.

To the best of our knowledge, there is no specific relaxation model described in the literature for the SD in the SmC phase. However, the relaxation model proposed by Vilfan and Žumer for the SD in smectic A phases[34] has been successfully used as an approximation in the analysis of experimental T_1^{-1} results in the SmC phase.[26] In the case where this relaxation mechanism is not dominant, its contribution to the relaxation rate can also be approximated by eq 2.[34]

(ii) Collective motions are described in nematic phases as 3-fold fluctuations of the director in laboratory axis frame and known as order director fluctuations (ODF). In smectic A phases, the viscoelastic properties are different

and splay elastic distortions reduce director fluctuations to layer undulations (LU).[25]

ODF and LU have clearly distinct T_1^{-1} dispersion profiles: $(T_1^{-1})_{\mathrm{ODF}} \sim \nu^{-1/2}$ and $(T_1^{-1})_{\mathrm{LU}} \sim \nu^{-1}$. These distinct profiles have been experimentally observed in many calamitic and tetrapode LC compounds.[25,26] The model equations for both ODF and LU can be expressed in general terms as

$$\left(\frac{1}{T_1}\right)_{\mathrm{C}} = A_{\mathrm{c}} \frac{1}{\nu^p}\left[f_{\mathrm{c}}\!\left(\frac{\nu_{\mathrm{Cmax}}}{\nu}\right) - f_{\mathrm{c}}\!\left(\frac{\nu_{\mathrm{Cmin}}}{\nu}\right)\right] \tag{3}$$

where c stands for ODF or LU and $p = 1/2$ or $p = 1$ for ODF or LU, respectively. The prefactor A_{c} is $A_{\mathrm{ODF}} = (C_{\mathrm{d}}k_{\mathrm{B}}TS^2\eta^{1/2})/(2\pi^{3/2}K^{3/2}a_{\mathrm{eff}}^{\,6})$ or $A_{\mathrm{LU}} = (C_{\mathrm{d}}k_{\mathrm{B}}TS^2)/(4\pi a_{\mathrm{eff}}^{\,6}LK)$, where L is the coherence length corresponding to the coherently fluctuating smectic layers and $a_{\mathrm{eff}}^{\,-6}$ depends on the interproton distances and interproton vectors' angles with respect to the long molecular axis. $f_{\mathrm{c}}(x)$ are dimensionless functions that reflect the high and low cutoffs observed in the T_1^{-1} dispersion profiles for frequencies above $\nu_{\mathrm{Cmax}} = 2\pi K(\eta l^2)$ and below $\nu_{\mathrm{Cmin}} = (2\pi K)/(\eta \xi^2)$, respectively. K is the elastic constant, considering a one-constant approximation,[35] and η is an average viscosity. l is the molecular length, and ξ is the coherence length associated with either the size of the nematic domain where order director fluctuations occur or the size of the smectic domain in a direction perpendicular to the layer's normal where layer undulations occur coherently.

In the smectic C phases the collective motions might be associated not only to layer undulations as in the case of SmA phases but also to in-plane fluctuations of the average tilt direction (TdF). This latter type of fluctuation has been detected in the SmC phase of a triphenyl LC system, and the relaxation model can also be expressed by three with $p = 1/2$ as in the case of ODF but with a different A_{c} prefactor.[31]

(iii) Local rotations/reorientations might be associated with both internal molecular motions or overall molecular motions. Usually, in low-resolution proton NMR the spin−lattice relaxation rate is not site-specific to a particular group of spins in the molecule but reflects the modulation of the dipolar spin interactions by the overall molecular motions. The correlation times of fast conformation changes in the chain(s) and core ring flips are usually in the range of 10^{-11}–10^{-12} s, whereas those of the global molecular rotational reorientations are much longer, sometimes in the range of 10^{-8}–10^{-11} s. In the case of molecules with more complex molecular structures, such as phasmidic, tetrapode, octapode, and dendrimer molecules, it was observed that due to the different correlation times, chain movements and global reorientation motions could be expressed by different contributions to T_1^{-1}.[26] Due to its particular molecular structure, rotations/reorientations of A131 might be described by a contribution from the chain motions expressed by the Bloembergen, Purcel, and Pound (BPP) model[36]

$$\left(\frac{1}{T_1}\right)_{\mathrm{Rch}} = A_{\mathrm{ch}}\left[\frac{\tau_{\mathrm{ch}}}{1 + \omega^2\tau_{\mathrm{ch}}^2} + \frac{4\tau_{\mathrm{ch}}}{1 + 4\omega^2\tau_{\mathrm{ch}}^2}\right] \tag{4}$$

with a prefactor, A_{ch}, and a single correlation time, τ_{ch}, for both A131 aliphatic chains. When considering this model on the analysis of the spin−lattice relaxation in ordered phases, this factor depends not only on the average interspin distances and angles ($A_{\mathrm{ch}} \propto C_{\mathrm{d}}/a_{\mathrm{eff}}^{\,6}$) but also on the degree of orientational order $\langle P_2 \rangle$ in the phase.

In view of the A131 bent-shape molecular core, the rotations/reorientations of this more rigid part of the molecule might be expressed by a model that considers restricted anisotropic rotational diffusions in a cone.[25] This motional model considers the A131 molecule as presented schematically in Figure 4. In this
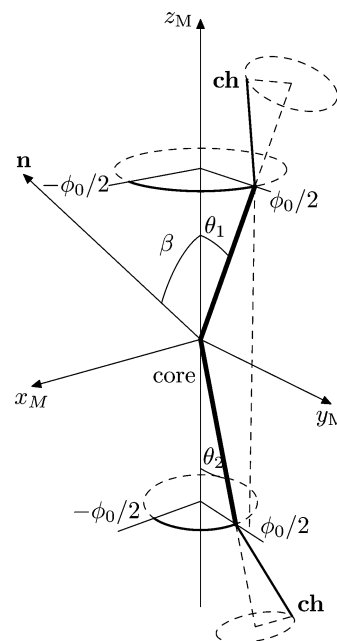
Figure 4. Schematic picture of the motional freedom of lateral arms and chains of A131 where ring c at the apex is assumed motionless; rings b, d, and e have the same angle θ_1; and ring a has angle θ_2 (see Figure 1).[37] The angles associated with the restricted rotational motions about the z_{M} axis are represented by $\pm \phi_0/2$ as explained in the text.

figure, the angles required by the model to describe the restricted rotations of the molecular core in the angle $\pm\phi_0/2$, around molecular axis z_{M}, are also presented.

Concerning the central benzene ring of the molecular core, the two lateral branches of the core might make angles θ_1 and θ_2, with respect to the z molecular axis, z_{M} (see Figure 4). These angles were estimated from previously reported ^{13}C chemical shifts and considered as temperature insensitive.[38] The molecule might perform librational motions with amplitude $\pm\phi_0/2$ around z_{M}. The chains, attached to the molecular core, might perform additional reorientations with correlation time τ_{ch} different from those of the molecular core.

The relaxation model for the restricted rotations can be expressed as

$$\left(\frac{1}{T_1}\right)_{\mathrm{Rco}} = A_{\mathrm{co}}[J_1(\omega) + J_2(2\omega)] \tag{5}$$

with $A_{\mathrm{co}} = C_{\mathrm{d}}/a_{\mathrm{eff}}^{\,6}$ and

$$
\begin{aligned}
J_p(p\omega) = \sum_{m=0}^{2} [d_{m,0}^{\,2}(\theta_i)]^2 \kappa_{pm}(\langle P_2\rangle, \langle P_4\rangle) \\
\times \Bigg[\frac{2(1 - \cos(m\phi_0))}{(m\phi_0)^2} \frac{\tau_{pm}}{1 + (p\omega\tau_{pm})^2} \\
+ 4\phi_0^2 \sum_{n=1}^{\infty} \frac{1 - (-1)^n\cos(m\phi_0)}{[(n\pi)^2 - (m\phi_0)^2]^2} \frac{m^2\tau_{pmn}}{1 + (p\omega\tau_{pmn})^2} \Bigg]
\end{aligned}
\tag{6}
$$

The correlation times τ_{pmn} and τ_{pm}, associated with the rotational diffusion modes considered in this model, are given by

$$\tau_{pm}^{-1} = \frac{D_\beta}{\beta_{pm}^2(\langle P_2 \rangle)} + p^2(D_\alpha - D_\beta) \qquad (7)$$

and

$$\tau_{pmn}^{-1} = \tau_{pm}^{-1} + \left(\frac{n\pi}{\phi_0}\right)^2 D_\phi \qquad (8)$$

where D_α, D_β, and D_ϕ are the diffusion coefficients corresponding to the precession of z_M about the director $\mathbf{n}$, molecular reorientations about a direction perpendicular to $\mathbf{n}$, and the restricted rotations about z_M, respectively. $d_{m,0}^2(\theta_i)$ values are the reduced Wigner matrices of second order. The kappa matrix $\kappa_{pm}(\langle P_2 \rangle, \langle P_4 \rangle)$ and functions $\beta_{pm}^2(\langle P_2 \rangle)$, in terms of second rank and four rank order parameters, can be found in the literature and are presented in the Supporting Information.[25]

In view of the models for the longitudinal relaxation mechanisms described above, n, d, τ_D, A_{ODF}, A_{LU}, ν_{Cmax}, ν_{Cmin}, A_{ch}, A_{co}, τ_{ch}, D_α, D_β, D_ϕ, $\langle P_2 \rangle$, $\langle P_4 \rangle$, and ϕ_0, angles θ_1 and θ_2 are the physical parameters that have to be considered and estimated from the analysis of the experimental results. Some of these parameters are temperature dependent. Since rotations/reorientations and translational self-diffusion are thermally activated relaxation mechanisms, the correlation times, τ_D and τ_{ch}, and diffusion coefficients, D_α, D_β, and D_ϕ, can be expressed in terms of Arrhenius-type expressions: $\tau_D = \tau_{D,T_{ref}} \exp[E_D R^{-1}(T^{-1} - T_{ref}^{-1})]$, $\tau_{ch} = \tau_{ch,T_{ref}} \exp[E_{ch} R^{-1}(T^{-1} - T_{ref}^{-1})]$, $D_{\alpha,\beta,\phi} = D_{\alpha,\beta,\phi,T_{ref}} \exp[-E_{\alpha,\beta,\phi} R^{-1}(T^{-1} - T_{ref}^{-1})]$, where E_D, E_{ch}, E_α, E_β, and E_ϕ are the activation energies, and $R \simeq 8.31$ J K^{-1} mol^{-1}. T_{ref} is the temperature used as a reference. The prefactors A_{ODF} and A_{LU} and cutoff frequencies ν_{Cmax} and ν_{Cmin} must also be considered temperature dependent. Since temperature dependence of the visco-elastic coefficients is unknown for A131, simple linear or quadratic polynomial dependences were considered. $\langle P_2 \rangle = (1 - T/T_{NI}^*)^\gamma$, with $\gamma \simeq 0.188$ and $T_{NI}^* \sim T_{NI} + 1$.[39] For the particular case of "rotational-diffusion-in-a-cone", $\langle P_2 \rangle$ and $\langle P_4 \rangle$ can be expressed in terms of the cone's semiangle (see the Supporting Information).[25]

Analysis of the Experimental Results. Eq 1 was fitted to the experimental results using a home-written nonlinear software package and considering a global minimum least-squares target.[40] The error estimates of the fitting parameters were obtained by considering the variation of the global least-squares target value with each one of the fitting parameters. For the sake of simplicity, the cross-dependence between the fitting parameter's errors was not considered. In view of the relaxation models used and the number of experimental results, several local least-squares minima could be obtained in the global minimization fitting procedure. The final fitting results include both available frequency and temperature dispersions in all the studied mesophases and correspond to the best fit which yields physically reasonable parameters. The model fitting parameters expressed at T_{ref} can be found in Table 1.
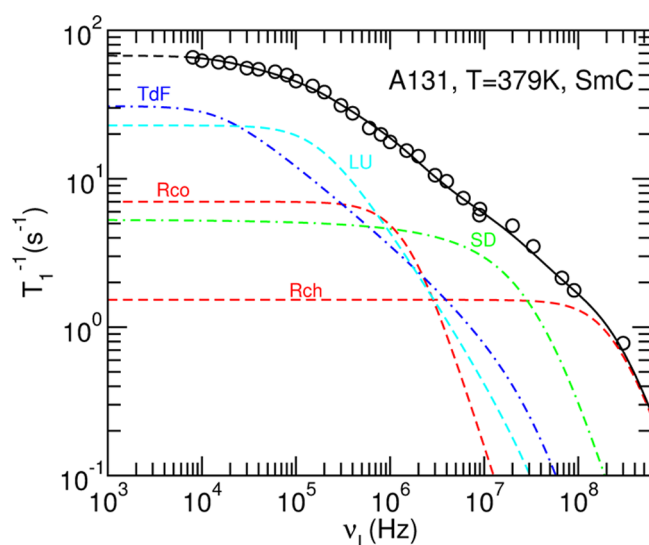
The experimental results and model fitting curves obtained for two temperatures in the N_u and N_x phases of A131 are presented in Figure 5. As it can be observed in that figure, the dispersion profiles in the nematic phases of A131 are well described by the proposed fitting model, and it is clear that order director fluctuations are dominant below the megahertz range. The T_1^{-1}
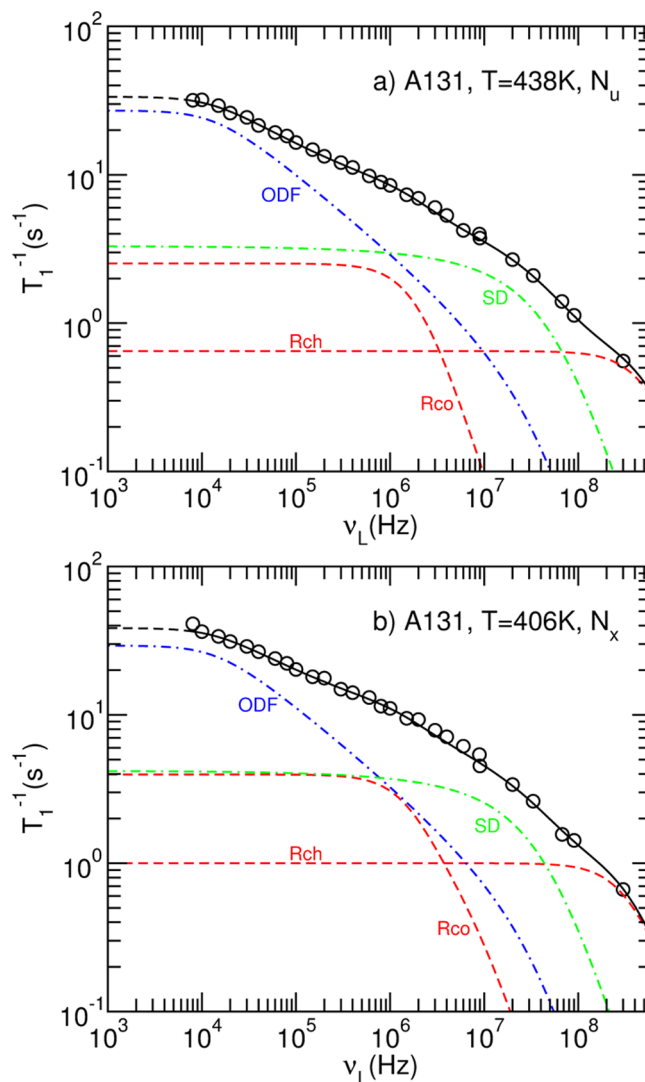
Figure 5. Experimental frequency dependent results and model fitting curves obtained for two temperatures in the nematic phases as explained in the text.

dispersion observed above 10 MHz has stronger contributions of the translational self-diffusion and fast chain rotations relaxation mechanisms. These T_1^{-1} dispersion profiles present some differences with respect to those observed in nematic phases of calamitic and tetrapode compounds.[30,31,41,42] The restricted rotations/reorientations relaxation contributions of Rco seem to represent a small correction to the total spin−lattice relaxation rate in the megahertz region in regard to the experimental results and fitting curves presented in Figure 5. However, the importance of this contribution becomes clear when analyzing all experimental results in a simultaneous fit, including both frequency and temperature T_1^{-1} dependences.

Figure 6 presents the T_1^{-1} dispersion results and model fitting curves obtained in the smectic C phase. The T_1^{-1} relaxation profile in the SmC phase should include layer undulations as expected, in view of the layered structure of this mesophase. The onset of layer order is expressed by a strong increase of T_1^{-1} with decreasing temperature and is well explained by the layers undulations' contribution to the total relaxation rate at all frequencies in Figure 6. However, it was clear that a better fit of the experimental data could only be obtained if a relaxation contribution, corresponding to in-plane fluctuations of the tilt

Figure 6. Experimental frequency dependent results and model fitting curves obtained for one temperature in the SmC phase as explained in the text.

Table 1. Model Parameters for $T = T_{ref} = 438$ K in the N_u Phase and $T = 406$ K in the N_x Phase Obtained from the Best Global Fit of Eq 1 to the Experimental T_1^{-1} Data[a]

	N_u	N_x
T (K)	438	406
τ_D ($\times 10^{-9}$)	1.79 ± 0.03	2.27 ± 0.03
D_α ($\times 10^7$ s^{-1})	1.19 ± 0.03	1.05 ± 0.03
D_β ($\times 10^4$ s^{-1})	12 ± 9	1.8 ± 1.4
D_ϕ ($\times 10^7$ s^{-1})	13 ± 3	0.022 ± 0.005
A_{co} ($\times 10^9$ s^{-2})	1.06 ± 0.02	
τ_{ch} ($\times 10^{-10}$)	1.53 ± 0.07	2.4 ± 0.1
A_{ch} ($\times 10^9$ s^{-2})	0.85 ± 0.03	
A_{ODF} ($\times 10^3$ s$^{-3/2}$)	3.43 ± 0.02	3.85 ± 0.03
ν_{Cmax} ($\times 10^6$)	~50	
$\langle P_2 \rangle$	~0.51	~0.65

[a]The remaining fitting parameters are E_D = 11.3 ± 0.8 kJ mol^{-1}, E_α = 5.0 ± 0.9 kJ mol^{-1}, E_β = 83 ± 68 kJ mol^{-1}, E_ϕ = 339 ± 10 kJ mol^{-1}, E_{ch} = 20.0 ± 0.9 kJ mol^{-1}, θ_1 = 20°, θ_2 = 30°, and ϕ_0 = 141 ± 3°. $A_{ODF} \simeq 9128 - 13T$. The low-cutoff frequency of ODF is $\nu_{Cmin} \simeq 24368 - 28.8T$ for T in the range of 377.5–449.5 K. A_{ch} and ν_{Cmax} were assumed to be constant with temperatures in the analyzed mesophases' temperature range of A131.

direction, was included in addition to LU, SD, Rco, and Rch. The presence of both types of collective motions was observed in other SmC phases.[31]

As can be seen in Table 1, the molecular core reorients based on the anisotropic viscosity model where D_α and D_β are diffusion coefficients with respect to the director frame, with tumbling (D_β) motions being 2 orders of magnitude smaller than its "precession" (D_α) motions around **n**. The amplitude of restricted rotation about z_M is 141°, which compares to ≃200° in the SmB phase of a calamitic LC.[43] Given the bent shape of A131, this ϕ_0 value in the nematic phase is not unexpected, and for simplicity it is fixed in all the nematic phases, while the corresponding diffusion coefficient, D_ϕ, yields a correlation time on the order of the chain's τ_{ch}, at the reference temperature. However, the activation energy, E_ϕ, is much larger than E_α, E_β, and E_{ch} activation energies, meaning that the librational ϕ motions become slower much

faster for lower temperatures than for the other rotational motions.

The A_{ODF} value is typical for nematic materials. The prefactor, A_{LU}, and low cutoff frequency, ν_{Cmin}, of the layer undulations mechanism were found to be strongly temperature dependent. In fact, $A_{LU} \simeq 22.5 + 3.753 \times 10^5 (390 - T) + 5289 (390 - T)^2$ and $\nu_{Cmin} \simeq 3.207 \times 10^5 - 5766 (390 - T) - 1032 (390 - T)^2$ in the temperature range of 377.5–391.7 K. A_{LU} increases as temperature decreases, and the low-cutoff frequency decreases with temperature as the result of a possible increase of viscosity or increase of the coherence length, ξ, or both.

In addition to the T_1^{-1} frequency dispersion plots, in Figure 7 are presented the T_1^{-1} temperature dependence data and model fitting curves obtained for four Larmor frequencies. The remaining plots can be found in the Supporting Information. As seen in this figure, the model used explains very well the main features of the experimental T_1^{-1} temperature dependences at all frequencies. These plots provide evidence for the relative influence of each relaxation mechanism at different frequencies. In the nematic phases $T_1^{-1}(T)$, profiles at 90 and 9 MHz are clearly dominated by the fast rotations/reorientations of the aliphatic chains and translation self-diffusion, respectively. The observed temperature dependences reflect the thermal activation character of these relaxation mechanisms, as proposed previously.

At 9 and 1 MHz the contribution of the restricted core rotations can also be observed, since the temperature dependence of $T_1^{-1}(T)_{Rco}$ clearly presents features that correspond to a slow dynamic regime. In fact, one can observe a $T_1^{-1}(T)_{Rco}$ maximum close to 407 K at 9 MHz in Figure 7 (top left panel) and an increase of $T_1^{-1}(T)$ for lower temperatures, as seen in the 1 MHz plot in Figure 7 (top right panel).

It would appear that the phase transition at around 422 K can be detected at a frequency of 9 MHz or nearby frequencies as a function of T, where the restricted core rotations play no role in the N_u phase but become significant to produce proton relaxation in the N_x phase. At 100 and 10 kHz, at around the same T, cusplike T dispersions have been detected.

In general, the quality of the fits in our relaxation model is quite good as seen in Figures 5–7. Nevertheless, the temperature dependent experimental results at 9 and 1 MHz and 10 kHz present some scattering that is not explained by the theoretical model considered. The T_1^{-1} cusplike fluctuations observed close to 422 K and data scattering for temperatures in the range 390–422 K might be associated to fluctuations of local order not considered in the models used. In particular the cusplike fluctuation observed close to 422 K in Figure 7 (bottom right panel) might be associated with changes in the viscoelastic parameters associated with conformation changes[18] or changes of packing ordering associated with different types of nematic order in the N_u and N_x phases, or both. The cusplike features at low frequencies were accounted for by additional ODF-like contributions, indicating that at low enough frequencies, certain director modes could sense local fluctuations as molecular packing conditions could change within a narrow region of the phase transition.

Based on previous ^{13}C data, the order parameters S and D for the V-shaped molecular core can be derived in which the twist angle of each ring(s) was used as an adjustable parameter. This gave the value of S at T_{ref} in Table 1. It was found that these twist angles are relatively insensitive to T except that of ring a.[38] In this case, the twist angle shows a gradual drop at around 422 K from a value of ~60° (above the N–N transition) to ~5° such that rings
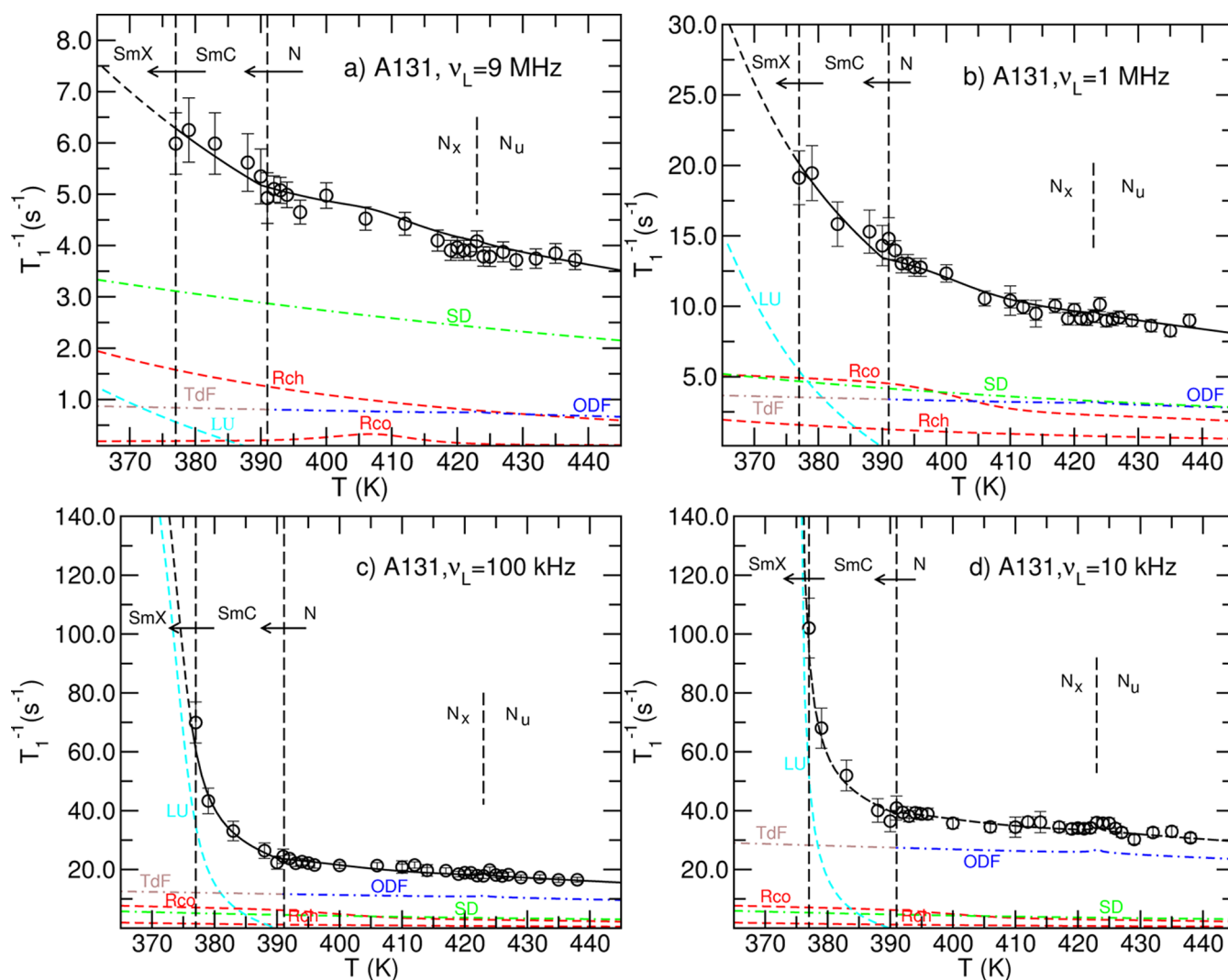
Figure 7. Experimental temperature dependent results and model fitting curves obtained for four Larmor frequencies as explained in the text: (a) ν_L = 9 MHz, (b) ν_L = 1 MHz, (c) ν_L = 100 kHz, and (d) ν_L = 10 kHz.

a and b become nearly coplanar in the N_x phase. In the vicinity of a phase transition, fluctuations in the conformational structures might induce an increase of viscosity as observed for other liquid crystals like 5CB.[44] Since $A_{ODF} \sim \eta^{1/2}$ (see previous section), an increase of η would correspond to an increase of the ODF pre-factor. Also, the low-cutoff frequency would decrease ($\nu_{Cmin} \sim \eta^{-1}$) producing an increase of the $(T_1^{-1})_{ODF}$ contribution at low frequencies.

CONCLUSIONS

A molecular dynamics study by proton NMR relaxation is presented in this work. The spin−lattice relaxation time was obtained in a broad frequency range from 8 kHz to 300 MHz for different temperatures in the nematic and smectic C phases of the A131 liquid crystal compound. In addition, T_1^{-1} temperature sweeps were obtained for selected frequencies. The T_1^{-1} experimental temperature sweeps point to changes in the molecular dynamics in the nematic phases of A131 in agreement with possible changes in packing of the average molecular conformer states.

The experimental results were analyzed taking into account a relaxation model that considers, in addition to collective motions and self-diffusion relaxation mechanisms, rotations/reorientations

of the aliphatic chains and restricted rotational-diffusion-in-a-cone relaxation mechanisms. A less detailed relaxation model for global rotations/reorientations failed to explain well the T_1^{-1} dispersion in the nematic N_x phase and the T_1^{-1} temperature dependence in the intermediate frequency range from 100 kHz to 9 MHz.

In the smectic C phase the collective motions relaxation mechanism was described by the sum of two types of relaxation contributions associated with layer undulations and in-layer fluctuations of the tilt direction (nematic-like contribution).

The simultaneous model fitting using a nonlinear least-squares minimization procedure to all experimental results was made possible after considering physically reasonable temperature dependences for the model parameters. The fitting parameters obtained from the best fits are in agreement with others found in the literature from other LC compounds. The model used, associated with the restricted rotations in a cone, was able to explain the main features of the experimental relaxation dispersion and T_1^{-1} temperature dependences, in particular in the intermediate frequency range.

In view of the relaxation model used, the more pronounced data scattering obtained around phase transition temperatures can be understood in terms of changes in the viscoelastic

constants that might result from different equilibrium intermolecular interactions associated with different average molecular conformer states. The strong slowing down of the molecular rotations around the bow axis of the A131 compound points to an increase of the molecular packing in the direction perpendicular to the bow axis, thus favoring an increase of local order along the secondary nematic director. Still, it is not possible to make inferences about the correlation length of this secondary order. Although the present proton relaxation study of A131 cannot distinguish the N_x phase between cybotactic-nematic and biaxial nematic,[45] it has affirmed a N−N transition in contrast to the report of Takezoe and co-workers.[17] The N−N_x transition is identified by a slowing down of the molecular rotations around the bow axis of the A131 compound, as detected in the T_1 dispersion analysis.

■ ASSOCIATED CONTENT

Ⓢ Supporting Information

Details of the A131 DSC, restricted rotational-diffusion-in-a-cone model, and additional fit plots. This material is available free of charge via the Internet at http://pubs.acs.org.

■ AUTHOR INFORMATION

Corresponding Author
*E-mail: pedro.jose.sebastiao@ist.utl.pt.

Notes

The authors declare no competing financial interest.

■ ACKNOWLEDGMENTS

■ REFERENCES

(1) *Physical Properties of Liquid Crystals*; Demus, D., Goodby, J. W., Gray, G. W., Spiess, H.-W., Vill, V., Eds.; Wiley-VCH: Weinheim, Germany, 1999.
(2) Prost, J.; Barois, P. *J. Chim. Phys. Phys.-Chim. Biol.* **1983**, *80*, 65−81.
(3) Niori, T.; Sekine, T.; Watanabe, J.; Furukawa, T.; Takezoe, H. *J. Mater. Chem.* **1996**, *6*, 1231−1233.
(4) Madsen, L. A.; Dingemans, T. J.; Nakata, M.; Samulski, E. T. *Phys. Rev. Lett.* **2004**, *92*, 145505.
(5) Lehmann, M.; Koehn, C.; Figueirinhas, J. L.; Feio, G.; Cruz, C.; Dong, R. Y. *Chem.—Eur. J.* **2010**, *16*, 8275−8279.
(6) Prasad, V.; Kang, S. W.; Suresh, K. A.; Joshi, L.; Wang, Q. B.; Kumar, S. *J. Am. Chem. Soc.* **2005**, *127*, 17224−17227.
(7) Figueirinhas, J. L.; Feio, G.; Cruz, C.; Lehmann, M.; Koehn, C.; Dong, R. Y. *J. Chem. Phys.* **2010**, *133*, 174509.
(8) Freiser, M. J. *Phys. Rev. Lett.* **1970**, *24*, 1041.
(9) Yu, L. J.; Saupe, A. *Phys. Rev. Lett.* **1980**, *45*, 1000−1003.
(10) Dong, R. Y. *Int. J. Mod. Phys. B* **2010**, *24*, 4641−4682.
(11) Luckhurst, G. R. *Thin Solid Films* **2001**, *393*.
(12) Lehmann, M. *Liq. Cryst.* **2011**, *38*, 1389−1405.
(13) Tschierske, C.; Photinos, D. J. *J. Mater. Chem.* **2010**, *20*, 4263−4294.
(14) Severing, K.; Saalw Achter, K. Phase Biaxiality in Nematic Liquid Crystals. In *Thermotropic Liquid Crystals: Recent Advances*; Ramamoorthy, A., Ed.; Springer: New York, 2007.
(15) Dong, R. Y.; Kumar, S.; Prasad, V.; Zhang, J. *Chem. Phys. Lett.* **2007**, *448*, 54−60.
(16) Dong, R. Y.; Marini, A. *J. Phys. Chem. B* **2009**, *113*, 14062−14072.
(17) Le, K. V.; Mathews, M.; Chambers, M.; Harden, J.; Li, Q.; Takezoe, H.; Jakli, A. *Phys. Rev. E* **2009**, *79*, 030701.

(18) Yoon, H. G.; Kang, S.-W.; Dong, R. Y.; Marini, A.; Suresh, K. A.; Srinivasarao, M.; Kumar, S. *Phys. Rev. E* **2010**, *81*, 051706.
(19) Senyuk, B.; Wonderly, H.; Mathews, M.; Li, Q.; Shiyanovskii, S. V.; Lavrentovich, O. D. *Phys. Rev. E* **2010**, *82*, 041711.
(20) Merkel, K.; Kocot, A.; Vij, J. K.; Korlacki, R.; Mehl, G. H.; Meyer, T. *Phys. Rev. Lett.* **2004**, *93*, 237801.
(21) Figueirinhas, J. L.; Cruz, C.; Filip, D.; Feio, G.; Ribeiro, A. C.; Frere, Y.; Meyer, T.; Mehl, G. H. *Phys. Rev. Lett.* **2005**, *94*, 107802.
(22) Tripathi, C. S. P.; Losada-Perez, P.; Glorieux, C.; Kohlmeier, A.; Tamba, M.-G.; Mehl, G. H.; Leys, J. *Phys. Rev. E* **2011**, *84*, 041707.
(23) Cestari, M.; Diez-Berart, S.; Dunmur, D. A.; Ferrarini, A.; de la Fuente, M. R.; Jackson, D. J. B.; Lopez, D. O.; Luckhurst, G. R.; Perez-Jubindo, M. A.; Richardson, R. M.; Salud, J.; Timimi, B. A.; Zimmermann, H. *Phys. Rev. E: Stat., Nonlinear, Soft Matter Phys.* **2011**, *84*, 031704.
(24) Panov, V. P.; Nagaraj, M.; Vij, J. K.; Panarin, Y. P.; Kohlmeier, A.; Tamba, M. G.; Lewis, R. A.; Mehl, G. H. *Phys. Rev. Lett.* **2010**, *105*, 167801.
(25) Dong, R. *Nuclear Magnetic Resonance of Liquid Crystals*; Springer: New York, 1997.
(26) Sebastião, P. J.; Cruz, C.; Ribeiro, A. C. Advances in Proton NMR Relaxometry in Thermotropic Liquid Crystals. In *Nuclear Magnetic Resonance Spectroscopy of Liquid Crystals*; Dong, R. Y., Ed.; World Scientific Publishing Co., Inc.: Hackensack, NJ, 2009; pp 129−167.
(27) Sousa, D. M.; Marques, G. D.; Cascais, J. M.; Sebastião, P. J. *Solid State Nucl. Magn. Reson.* **2010**, *38*, 36−43.
(28) Noack, F. *Prog. Nucl. Magn. Reson. Spectrosc.* **1986**, *18*, 171−276.
(29) Kimmich, R.; Anoardo, E. *Prog. Nucl. Magn. Reson. Spectrosc.* **2004**, *44*, 257−320.
(30) Sebastião, P. J.; Gradišek, A.; Pinto, L. F. V.; Apih, T.; Godinho, M. H.; Vilfan, M. *J. Phys. Chem. B* **2011**, *115*, 14348−14358.
(31) Carvalho, A.; Sebastião, P. J.; Ribeiro, A. C.; Nguyen, H. T.; Vilfan, M. *J. Chem. Phys.* **2001**, *115*, 10484−10492.
(32) Žumer, S.; Vilfan, M. *Phys. Rev. A* **1978**, *17*, 424−433.
(33) Torrey, H. C. *Phys. Rev.* **1953**, *92*, 962−969.
(34) Vilfan, M.; Žumer, S. *Phys. Rev. A* **1980**, *21*, 672−680.
(35) de Gennes, P.; Prost, J. *The Physics of Liquid Crystals*, 2nd ed.; Oxford University Press: New York, 1993.
(36) Bloembergen, N.; Purcell, E. M.; Pound, R. V. *Phys. Rev.* **1948**, *73*, 679−712.
(37) Gonçalves, L. N. MetaPost macros for 3D; http://www.ctan.org/pkg/featpost.
(38) Dong, R. Y. *Encyclopedia of Analytical Chemistry*; to be published.
(39) Haller, I. *Prog. Solid State Chem.* **1975**, *10*, 103−118.
(40) Sebastião, P. J. 2009; http://fitteia.ist.utl.pt.
(41) Filip, D.; Cruz, C.; Sebastião, P. J.; Cardoso, M.; Ribeiro, A. C.; Vilfan, M.; Meyer, T.; Kouwer, P. H. J.; Mehl, G. H. *Phys. Rev. E: Stat., Nonlinear, Soft Matter Phys.* **2010**, *81*, 011702.
(42) Apih, T.; Domenici, V.; Gradišek, A.; Hamplova, V.; Kaspar, M.; Sebastião, P. J.; Vilfan, M. *J. Phys. Chem. B* **2010**, *114*, 11993−12001.
(43) Shen, X.; Dong, R. Y. *Mol. Phys.* **1994**, *83*, 1117−1131.
(44) Chmielewski, A. G.; Lepakiewicz, E. *Rheol. Acta* **1984**, *23*, 207−210.
(45) Keith, C.; Lehmann, A.; Baumeister, U.; Prehm, M.; Tschierske, C. *Soft Matter* **2010**, *6*, 1704−1721.